PHYSICAL REVIEW E **84**, 041809 (2011)

Coil-bridge transition and Monte Carlo simulation of a stretched polymer

Jeff Z. Y. Chen
Department of Physics and Astronomy, University of Waterloo, Waterloo, Ontario, Canada N2L 3G1

(Received 5 July 2011; published 25 October 2011)

The structure of the system consisting of a grafted self-avoiding polymer chain attracted to the surface layer of a flat wall at a distance away by a short-ranged force is investigated. A first-order transition is determined between the coil state at a low attraction energy and the bridge state at a high attraction energy. The transition properties of the system are obtained by a Monte Carlo simulation, which uses the inverse density of states as the transition weight and is reweighted back to a canonical ensemble. The determination of the density of states follows a revised Wang-Landau procedure in which the center-of-mass distance from the grafted site is used as the variable. Scaling arguments are also given for the observed numerical results.

DOI: 10.1103/PhysRevE.84.041809 PACS number(s): 82.35.Gh, 68.35.Rh, 64.60.De, 61.41.+e

I. INTRODUCTION

Consider a polymer that has one terminal end grafted to a fixed site in space and is otherwise unconstrained. At a distance H away is an attractive potential well with magnitude u, adjacent to a hard wall (see Fig. 1). An interesting case is the system where H is greater than the radius of gyration of the grafted polymer—the polymer needs to be in an extended conformation to reach the attractive surface, which is not desirable by the conformation entropy of a free polymer. At a large u, the polymer forms an extended state [Fig. 1(b)] where the stem portion of the polymer is greatly stretched from a coil state and the other portion is located near the attractive wall surface. Leermakers and Gorbunov called this transition the coil-bridge transition and worked out a scaling theory based on the Gaussian statistics of the polymer conformation [1]. In the present paper, the properties of the coil-to-bridge transition of a polymer chain that incorporates more realistic physical features, such as the excluded-volume effect between monomers and finite chain extensibility, are considered.

Experimentally, the dependence of the phase diagram [Fig. 1(c)] on H can be probed by moving either the flat surface or the grafting point. With a relatively strong reduced binding energy βu, where $\beta = 1/k_B T$ with k_B being the Boltzmann constant and T the temperature, one can access the bridge state by varying H, crossing the coil-bridge transition boundary. This can be done similar to, for example, atomic force microscopy experiments that manipulate a single polymer chain [2–7]. Most of these experiments focused on the elastic properties of a polymer after the chain has already been adsorbed or attached to the surface of two separating or approaching surfaces. There is a need for direct experimental investigation of the coil-bridge transition near the vicinity of the transition. One of the interesting results from the scaling prediction is that at the transition, the fraction of monomers attracted to the surface is directly related to the universal scaling exponent for the radius of gyration, for a system where H is much less than the polymer contour length.

This paper serves two purposes: illustrating the first-order coil-bridge transition and introducing a Monte Carlo procedure suitable for studying a highly stretched polymer system. Using Monte Carlo simulation results (Sec. III A) and scaling theories (Appendixes), we describe the basic conformational properties of the system and determine the phase diagram. The fraction of monomers adsorbed to the surface area *jumps discontinuously* at the coil-bridge transition. Accompanying the first-order transition, a free energy barrier, caused by stretching the polymer over the region, needs to be overcome, as discussed in Sec. III. If the jump is large, one would expect a hysteresis effect in a real system: crossing the phase boundary by varying H from the high end and from the low end produces apparently different transition points. These properties can be contrasted to the findings from a recent Monte Carlo simulation on a very similar system by Bhattacharya and coworkers, where a phase diagram similar to Fig. 1(c) was drawn and the transition was considered "pseudo" continuous [8].

The encountered difficulty of using a normal Monte Carlo procedure in systems with conformational free-energy traps separated by a high barrier is well known; one needs to resort to other Monte Carlo tricks to faithfully map out the distribution functions of an appropriate order parameter [9,10]. Take the current system for example. There is a high entropic cost to stretch the free end of the polymer to the vicinity of the attracting wall surface—this particular conformation is an intermediate state, which must be experienced by the polymer in the simulation before the adsorption takes place. Associated with the intermediate state is a free-energy barrier, of the magnitude $\beta E_b \sim (H/R_g)^{5/2}$ (see Sec. III C) estimated from a scaling argument [11], where R_g is the radius of gyration of a free polymer. Because we are mostly interested in the parameter regime $H/R_g \geqslant 1$, in a normal Monte Carlo simulation, the occurrence of such a conformation is exponentially rare.

Recent years have witnessed a rapid growth in Monte Carlo simulations that use non-Boltzmann transitional probabilities, which enable better sampling of the low-energy area of a rough energy landscape. One particularly useful technique is the Wang-Landau method that yields the density of state for a given energy in a high precision; the inverse of the resulting density of state can then be used as a transitional probability in a Monte Carlo simulation, which allows a random walk of the simulated system in the energy space and overcomes the free-energy barrier problem. The success of the Wang-Landau method is well documented in the literature [12,13].

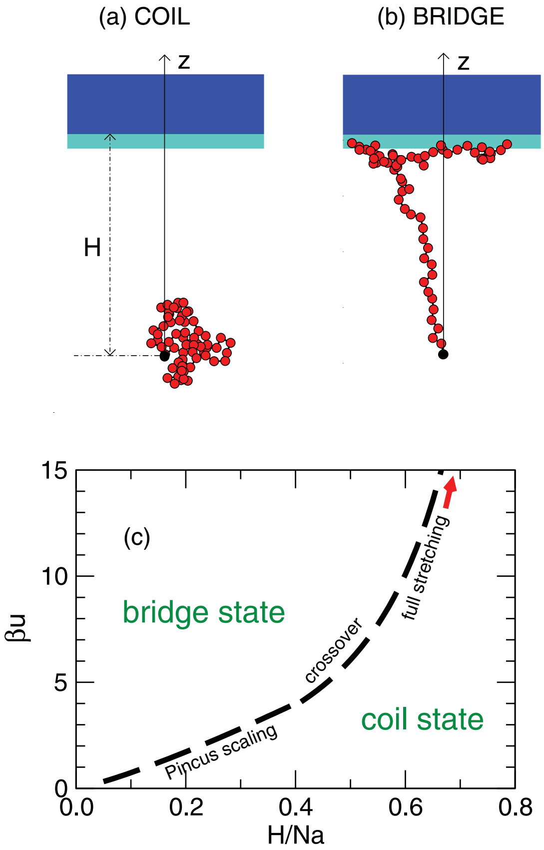

FIG. 1. (Color online) Snapshots of the simulated system in a (a) coil (desorbed) or (b) bridge (adsorbed) state, and the expected phase diagram (c). Circles (red) in (a) and (b) represent a self-avoiding polymer and the black circle a fixed terminal monomer at the origin. The dark shaded area (deep blue) represents a hard wall, and a light shaded region (light blue) indicates an attractive potential well of force range a, inside of which a monomer loses an energy u. The example shown in (a) and (b) has a ceiling-height/polymer-length ratio $H/Na = 0.6$ and number of polymer bonds $N = 64$.

A naive application of the Wang-Landau method to the current simulation system would be using the total adsorption energy as the weight variable. This, however, does not solve our problem, as the difficulty we have is mostly caused by the conformation entropy. In this paper, we propose to use the z coordinate of the center of mass of the polymer, Z, as the weighting variable (see Sec. II A). The two concerned states, a coil state and a perfect bridge, separately correspond to $Z = 0$ and $Z = Z_m$, where the latter corresponds to a perfect, T-shaped bridge conformation. The location of the free-energy barrier is approximately at $Z = H/2$, also well characterized by Z. Once the density of state of Z is determined, the simulated system conducts a random walk in the Z space, yielding adequate statistics covering the entire Z region. On the basis of the collected statistics, we can either deduce the thermal average that entails the inclusion of a canonical weight in the simulation measurement (see Secs. II B and III A), or use the resulting Z-dependent free energy that directly displays the double-well structure expected in a first-order transition (see Secs. III B and III C).

II. MODEL AND SIMULATION

A. Determination of the density of state

A self-avoiding polymer was modeled as a three-dimensional chain of N bonds each having length a, with the first monomer fixed to the origin. Every monomer has a hard-sphere diameter $d = 0.9a$. At a Monte Carlo (MC) trial, a randomly selected monomer was rotated about the vector connecting the two adjacent monomers along the chain, subject to the excluded-volume conditions between the monomers as well as between the selected monomer and the flat hard wall at $z = H$. The acceptance of such an attempt was evaluated based on the Metropolis algorithm [14] for the statistical weight $W(Z) = 1/g(Z)$ where Z is the z coordinate of the center of mass of the entire polymer chain and $g(Z)$ is its density of states. Note that at this stage, the effect of the potential well near the wall does not enter into a simulation attempt; but it will be considered in the measurement formalism as described in the next section.

Consider a system with specified N and H. The determination of $g(Z)$ exactly followed the prescription given by Wang and Landau, except for the usage of Z as the reference parameter, not energy as in their original work [12]. The range of variation for the center-of-mass coordinate Z was assumed to be within $[0, Z_m]$ where Z_m corresponds to a perfect bridge state; in such a state, the stem segment of the polymer is straight, lying along the positive z axis, and all other monomers are located at $z = H - a/2$ inside the potential well [light shaded (light blue) area in Fig. 1]. The Z range was evenly divided into $m = 1000$ bins, where the function $g(Z)$ for the ith bin is represented by a variable $g_i (i = 1,2,3,\ldots,m)$. An initial guess, $\ln g_i = 1$ for all i, was made to start the $g(Z)$-determination process, together with a step size $h = 1$ to be used below.

The next step was to run a MC simulation segment such that the array $\ln g_i$ was updated at every Monte Carlo attempt, by $\ln g_i \leftarrow h + \ln g_i$, once the polymer's center-of-mass settled in the ith bin. A new approximation for the Monte Carlo weight $W(Z) = 1/g(Z)$ was then obtained for that bin. The histogram for the number of times that a bin was visited, K_i, was collected from this MC segment. A simulation segment was terminated when the maximal relative difference $|K_i - \bar{K}|/\bar{K}$, where $\bar{K}$ is the average of all K_i, is less than 20%. The step size h was then multiplied by $1/2$ and a new MC simulation segment was conducted by using the new h.

Thus, every new MC segment had a new h which was half of what was used in the previous segment. The iteration of MC segments was considered convergent after h became smaller than 10^{-8}. An approximation for $\ln g(Z)$ was then obtained. Examples of $\ln g(Z)$ are plotted as functions of Z in the upper panels of Fig. 2, for a few selected values of N and H. In each case, ten independent estimates for $\ln g(Z)$ were obtained; based on these, the relative error $\Delta g(Z)/g(Z)$ for $g(Z)$, or the absolute error $\Delta[\ln g(Z)]$ for $\ln g(Z)$, was estimated, shown in the lower panels of Fig. 2.

B. Production run

The measurements in a canonical ensemble $[N, H, \beta u]$ were obtained from the production run by including the Boltzmann

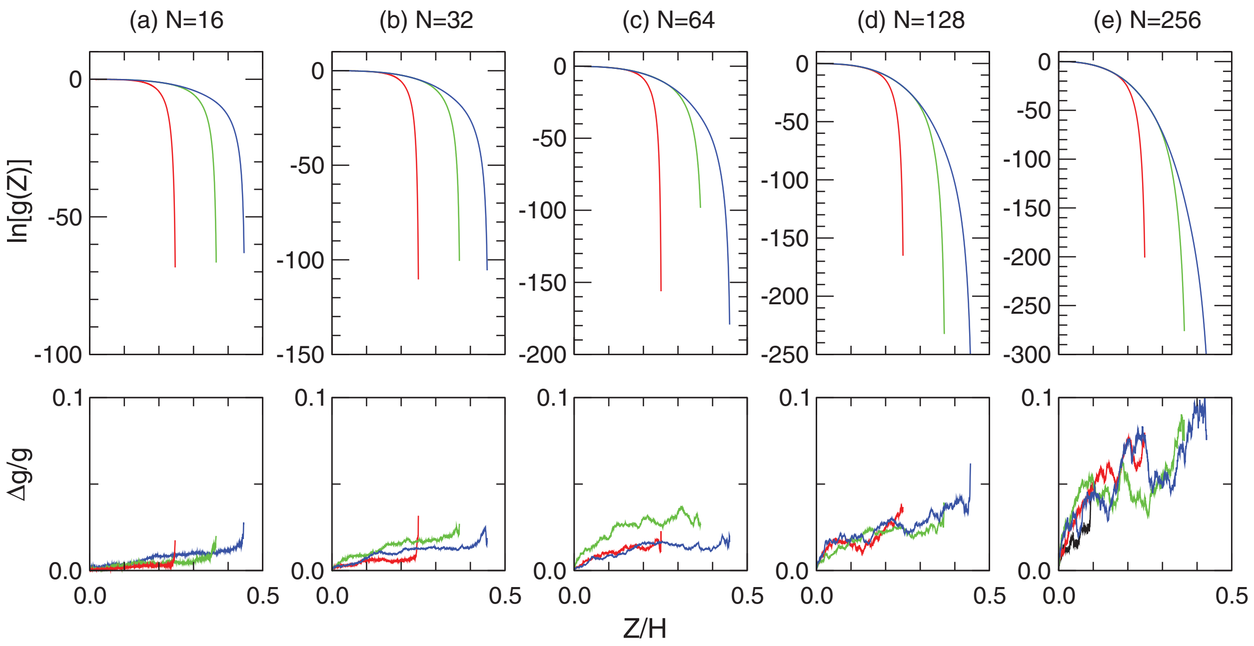

FIG. 2. (Color online) Density of states $g(Z)$ as a function of the polymer's center-of-mass height Z in a logarithmic plot (upper panels) and its relative error $\Delta g/g = \Delta[\ln g(Z)]$ (lower panels), for (a) $N = 16$, (b) $N = 32$, (c) $N = 64$, (d) $N = 128$, and (e) $N = 256$, produced from the Wang-Landau Monte Carlo determination. In each $g(Z)$ plot, from left to right, example curves correspond to $H/a = 0.3$ (red), 0.5 (green), and 0.7 (blue). In all plots, $g(Z)$ has been normalized by a constant such that $g(0) = 1$.

factor in the measurement. In this paper, a symbol with an overbar, $\overline{A}(\beta u)$, denotes the average of a physical quantity A in a canonical ensemble,

$$\overline{A}(\beta u) = \frac{\int d(\cdot)A(\cdot)\exp[-\beta u V(\cdot)]}{\int d(\cdot)\exp[-\beta u V(\cdot)]}, \tag{1}$$

where the abbreviation $(\cdot)$ is used for all variables that describe the positions of all movable monomers of the grafted polymer. The reduced total potential energy was calculated from

$$V(\cdot) = \sum_{i=1}^{N+1} v(z_i), \tag{2}$$

where $v(z_i)$ is the reduced potential energy experienced by the ith monomer having the Cartesian coordinates (x_i, y_i, z_i),

$$v(z_i) = \begin{cases} -1 & \text{if } \ H - a < z_i \leqslant H, \\ \infty & \text{if } \ H < z_i, \\ 0 & \text{otherwise.} \end{cases} \tag{3}$$

The potential-well depth u has been factored out explicitly in these expressions to demonstrate the scaling of variables.

For any given polymer configuration described by the coordinates $(\cdot)$ we can define the z coordinate of the center of mass

$$\zeta(\cdot) = \frac{1}{N+1}\sum_{i=0}^{N+1} z_i. \tag{4}$$

In fact, during a MC production run, the measured histogram of visited Z is related to

$$H(Z) = \int d(\cdot)W[\zeta(\cdot)]\delta[Z - \zeta(\cdot)], \tag{5}$$

where δ is Dirac's delta function. Because the density of states for Z is defined by

$$g(Z) = \int d(\cdot)\delta[Z - \zeta(\cdot)], \tag{6}$$

in a production run where $W(\zeta) = 1/g(\zeta)$ is used as a statistical weight, $H(Z)$ reaches a Z-independent constant after adequate statistics. The advantage of using $1/g(\zeta)$ as the transition probability in a MC simulation is that the simulated polymer goes through coil (low Z) and stretching (high Z) states multiple times within a production run.

We can then rewrite Eq. (1) as

$$\overline{A}(\beta u) = \frac{\int_0^{z_m} dZ g(Z)\langle A(Z,\beta u)\rangle}{\int_0^{z_m} dZ g(Z)\langle Q(Z,\beta u)\rangle}, \tag{7}$$

where

$$\langle A(Z,\beta u)\rangle \equiv \frac{\int d(\cdot)W[\zeta(\cdot)]A(\cdot)\exp[-\beta u V(\cdot)]\delta[Z - \zeta(\cdot)]}{\int d(\cdot)W[\zeta(\cdot)]\delta[Z - \zeta(\cdot)]}, \tag{8}$$

and

$$\langle Q(Z,\beta u)\rangle \equiv \frac{\int d(\cdot)W[\zeta(\cdot)]\exp[-\beta u V(\cdot)]\delta[Z - \zeta(\cdot)]}{\int d(\cdot)W[\zeta(\cdot)]\delta[Z - \zeta(\cdot)]}. \tag{9}$$

In a production run, the left-hand side of Eq. (8) was collected in a two-dimensional array, one of the index dealing with the bin number for Z and the other for a set of prespecified values βu. For a given set, Z and βu, the value $\langle A(Z,\beta u)\rangle$ was derived from a simple algebraic average of all measured $A(\cdot)\exp[-\beta u V(\cdot)]$. The average $\langle Q(Z,\beta u)\rangle$ was obtained similarly, but now only the factor $\exp[-\beta u V(\cdot)]$ was measured.

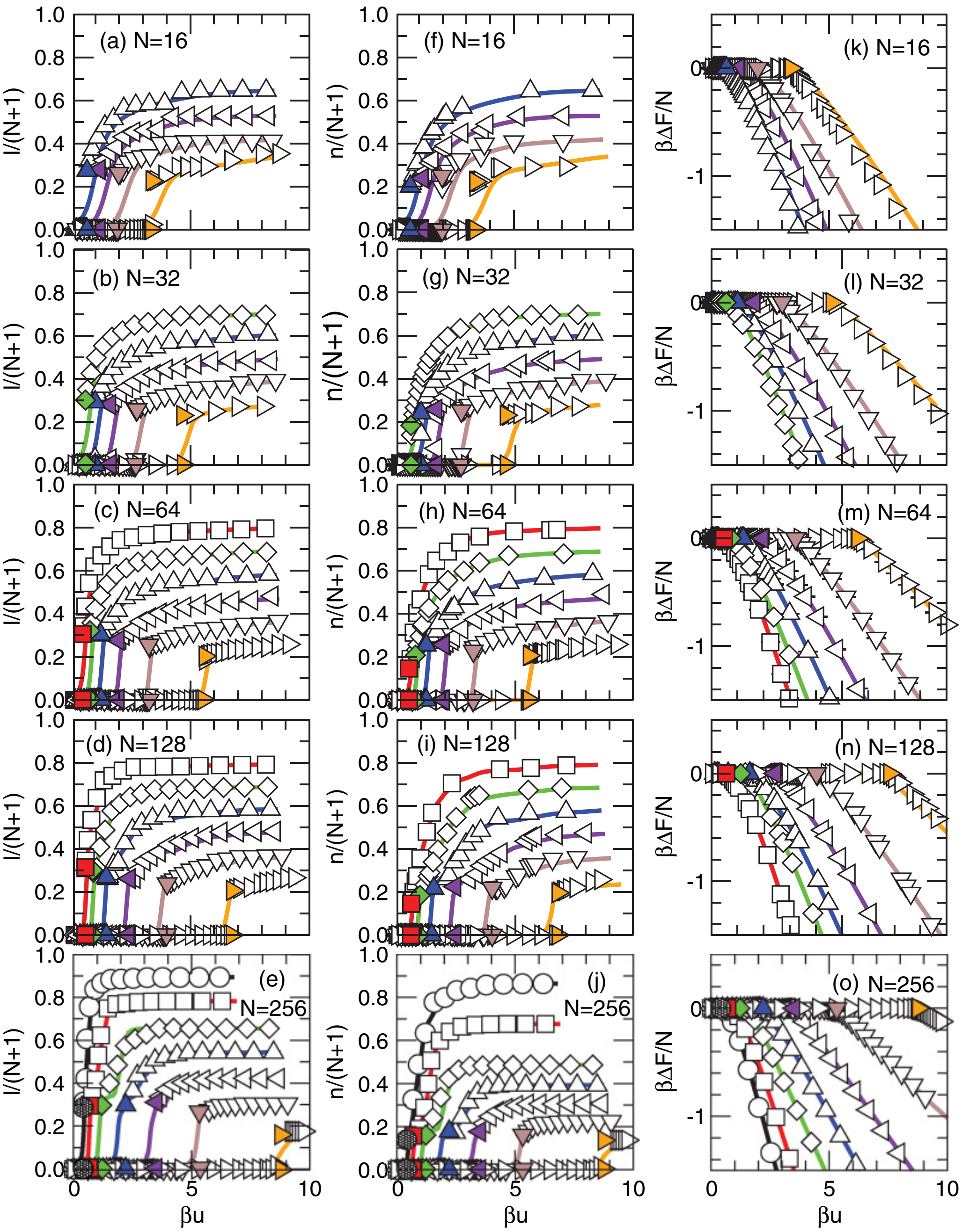

FIG. 3. (Color online) Simulation results for the fraction of monomers near the wall $\bar{l}/(N+1)$ [plots (a)–(e)], fraction of monomers inside the potential well $\bar{n}/(N+1)$ [(f)–(j)], and the free-energy difference per bond by using the coil state as the reference $\beta\Delta F/N$ [(k)–(o)], as functions of the reduced adsorption energy βu. Each curve in these plots corresponds to a specific ratio between the grafting-point to wall-surface distance H and the total polymer contour length Na: right triangles and the underlying curves (orange) represent $H/Na = 0.7$, down triangles and the underlying curves (brown) $H/Na = 0.6$, left triangles and the underlying curves (purple) $H/Na = 0.5$, up triangles and the underlying curves (blue) $H/Na = 0.4$, diamonds and the underlying curves (green) $H/Na = 0.3$, squares and the underlying curves (red) $H/Na = 0.2$, and circles and the underlying curves (black) $H/Na = 0.1$. Curves were produced from production runs based on the thermal-average formalism defined in Eq. (7); symbols were produced from the Z-dependent energy analysis introduced in Sec. III B. Filled symbols indicate the location of the projected coil-bridge transition.

It is possible to directly probe the free energy of the system from this Monte Carlo method. Within a constant (β-independent) prefactor the partition function can be calculated,

$$Q(\beta u) = \int_0^{Z_m} dZ g(Z)\langle Q(Z,\beta u)\rangle. \tag{10}$$

The free-energy difference of the system, in reference to the free energy in a desorbed state ($\beta u = 0$), is defined by

$$\beta\Delta F(\beta u) = -\ln[Q(\beta u)/Q(0)]. \tag{11}$$

Hence, for a given system (that is, a given set of N and H/Na), the entire βu dependence of a measurable in the $[N,H,\beta u]$ ensemble can be obtained within one single production. In this work, a Monte Carlo step (MCS) is defined as N MC trials; a production run consisted of 10^9 MCS and was split among multiple processors for parallel computation. The production run was approximately 10^2 longer than needed; 10^7 was actually adequate for producing a reasonably accurate $\overline{A}$, which is presented in the next section, represented by thick curves in the plots. A well characterization of the Z-dependent free energy (see Sec. III B), which is a better tool for analyzing the first-order nature of the coil-bridge transition, requires more statistics to fill the multiple bins dividing the Z variable (which is the reason for 10^2 times more statistics); a data point produced from this analysis is represented by a symbol in the plots.

III. SIMULATION RESULTS

A. Thermal average

Within the present model, any thermal average of a physical quantity depends on three parameters: the number of monomers in a chain $N+1$, the distance between the grafted end and the attractive surface reduced by the total polymer length H/Na, and the magnitude of the potential well reduced by a β factor βu. The calculated physical properties are shown by smooth curves behind symbols in Fig. 3, where each value of H/Na is represented by a different color. The figure displays three physical measurements as functions of βu: the average fraction of monomers near the adsorption surface $\bar{l}/(N+1)$, the average fraction of monomers that are inside the potential well $\bar{n}/(N+1)$, and the total free energy calculated based on Eq. (11). For a given configuration, the number of stem monomers m was measured by counting the monomers from the grafted end to the first adsorbed monomer; then, l was deduced from $l = N + 1 - m$.

A typical curve in Fig. 3 starts from 0, corresponding to the coil state in the low-βu region where no monomer-surface contact is made, *smoothly* increases in a transitional region, and approaches a plateau [in plots (a)–(j)] or a straight line [in plots (k)–(o)], corresponding to the bridge state in the high-βu region. Because of the finite-size effects, we cannot distinctively observe the abrupt jump predicted in the Appendixes for a first-order phase transition, from the smoothly varying curves in plots (a)–(j). One useful feature is that the transition region narrows as we examine the sequence of plots from low N to high N. In the current free-energy plots, (k)–(o), the portion of curves in the transition region is blocked by symbols; an enlarged version of these plots shows smoothly varying curves, which is different from the expectation that at the first-order transition, two branches of free energy cross each other by straight lines.

In a recent Monte Carlo simulation where the Boltzmann weight was directly used, curves similar to plots in Figs. 3(f)–3(i) were obtained. The smoothness of these curves has made Bhattacharya and coworkers to claim that the transition is “pseudo” continuous [8], rather than discontinuous. As demonstrated in the next section, the first-order nature can be readily extracted from the current Monte Carlo simulation that uses an inverse density of state as a simulation weight. The results are demonstrated in the plots by symbols.

B. *Z*-dependent free energy

The Z-dependent partition function $\langle Q(Z,\beta u)\rangle$ defined in Eq. (9) carries the physical meaning of (un-normalized) probability of finding the z coordinate of the polymer’s center of mass in the immediate region about Z. The corresponding free-energy difference can be defined as

$$\beta\Delta F(Z,\beta u) = -\ln[\langle Q(Z,\beta u)\rangle/\langle Q(0,\beta u)\rangle], \tag{12}$$

which is a function of both Z and βu. In a coil state, we expect that on average the center of mass of the polymer coincides with the grafting site, hence $\beta F(Z,\beta u)$ has a minimum at $Z = 0$. On the other hand in a bridge state, the polymer is stretched, hence we expect to see a free-energy minimum at a relatively large Z. From the examination of the Z-dependent free energy $\beta F(Z,\beta u)$ emerges an in-depth tool for analyzing the first-order nature of the coil-bridge transition.

Figure 4 shows examples of numerical results of $\beta\Delta F(Z,\beta u)$ for $N = 64$. At a lower βu, when the system is in a coil state, there is a global minimum at $Z^* = 0$ (upper curves); at a higher βu when the system is in a bridge state, there is a global minimum at a large Z^*/H (lower curves). The location of the minimum is normally greater than $1/2$ in Z/H; in a strongly stretched polymer, as the segment near the free end of the polymer reaches the adsorbing surface, the center of mass is slightly above the halfway of the entire stretch.

Our identification of the location of minimum Z^* for a given βu allows us to define the measurement of a physical property, represented in Eq. (8), at the minimum,

$$A^*(\beta u) \equiv \langle A(Z^*,\beta u)\rangle. \tag{13}$$

The numerical determination of $l^*(\beta u)$ and $n^*(\beta u)$, together with the free-energy minimum,

$$\Delta F^*(\beta u) \equiv F(Z^*,\beta u), \tag{14}$$

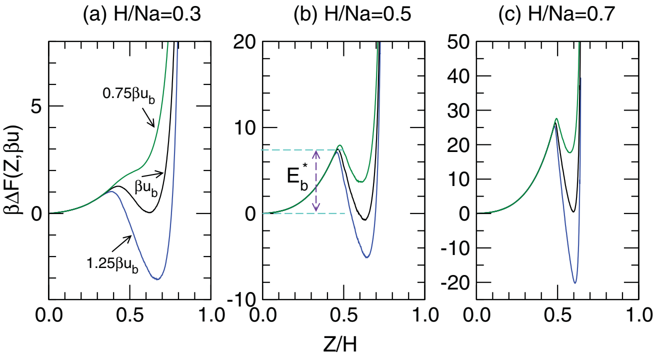

FIG. 4. (Color online) Reduced free energy $\beta\Delta F(Z,\beta u)$ as a function of the polymer’s center-of-mass height Z for $N = 64$ in three cases: (a) $[H/Na = 0.3, \beta u_\mathrm{b} = 0.77]$, (b) $[H/Na = 0.5, \beta u_\mathrm{b} = 0.2]$, and (c) $[H/Na = 0.7, \beta u_\mathrm{b} = 5.6]$. In each plot, three curves are generated, corresponding to $\beta u = 0.75\beta u_\mathrm{b}$, βu_b, and $1.25\beta u_\mathrm{b}$, from top (green), middle (black), to bottom (blue), respectively. Here, βu_b is the reduced transition energy of the first-order coil-bridge transition. An energy barrier height E_b^* is indicated in plot (b).

are represented in Fig. 3 by various open symbols overlaying the curves. In parameter regions where the Z-dependent free energy has a sharp minimum, l^*, n^*, and F^* all agree well with the thermal average $\bar{l}$, $\bar{n}$, and F represented by the underlying curves in the figure. This usually happens in a "deep" coil or "deep" bridge state, far away from the coil-bridge transition region. Near the transition point where fluctuations about the free-energy minimum are significant, the difference between l^* and $\bar{l}$ (the deviation of symbols from curves) is visible in the plots.

C. Transition point

The number of monomers near the adsorbing surface, l^*, has a value $l^* = 0$ in the coil state and makes a jump to a finite value $l^*_{\rm b}$ in the bridge state at a reduced transition adsorption energy, $\beta u_{\rm b}$. This is shown in Figs. 3(a)–3(e) by filled symbols at the transition. Any physical property in a bridge state at the coil-bridge transition is denoted by a subscript b in this paper.

The data for $l^*_{\rm b}$, together with the error bars estimated from ten separate runs, is plotted in Fig. 5(a) as a function of H/Na. The second row of Table I summarizes results from simple scaling theories, presented in the Appendixes for an $N \to \infty$ system. We see that $l^*_{\rm b}/N$ is a universal constant in the $H/aN^\nu \gg 1$ region. A Gaussian-chain model predicts a universal value 1/2, but a self-avoiding-chain model, which the current simulation should follow, predicts a universal value indicated by the long-dashed line in the plot. These scaling predictions are valid in the parameter region $H \ll Na$, where the effects of the finite extension of a polymer chain (Na) are not considered. Symbols in Fig. 5(a) represent the simulation results and are classified according to the extent of stretching: filled symbols are for extended systems ($H/Na = 0.6, 0.7$), shaded symbols for relatively less extended systems ($H/Na = 0.4, 0.5$), and open symbols are closer to the $H \ll Na$ limit ($H/Na \leqslant 0.3$).

The circles ($N = 256$) approach the long-dashed line in the small H/Na regime, but the agreement is not completely satisfactory. Note that even the largest-N system simulated in this work has only approximately $l^*_{\rm b} \sim 30\% N \sim 75$ monomers in the vicinity of the adsorbing surface. For such a low l^*, the validity of the scaling form for the adsorption free energy assumed in Appendix A, i.e., the second term in Eq. (A1), is undoubtedly questionable [15,16]. The universal scaling-theory predication in Eq. (A5), $l_{\rm b}/N = 0.411$, is valid when the following conditions are simultaneously met:

$$N^\nu \ll H/a \ll N. \tag{15}$$

While the scaling-theory prediction is produced from well-grounded and well-tested pieces of free-energy contributions, it remains to be tested directly by computer simulations of a much larger-N system that meet these requirements, for the coil-bridge transition.

Another important feature of the data in Fig. 5(a) is that $l^*_{\rm b}/(N+1)$ starts to decrease as H/Na becomes relatively large (e.g., see filled symbols in the plot). In this case, the free energy of the stretched segment does not follow the Pincus scaling and the data points move away from the expected universal line. In Appendix B, using a qualitative expression for the free energy, we predict how $l_{\rm b}/N$ varies as a function of H/Na near the full-stretching limit. We can see a reasonable agreement between the filled data and the dot-dashed curve representing the function in Eq. (B4).

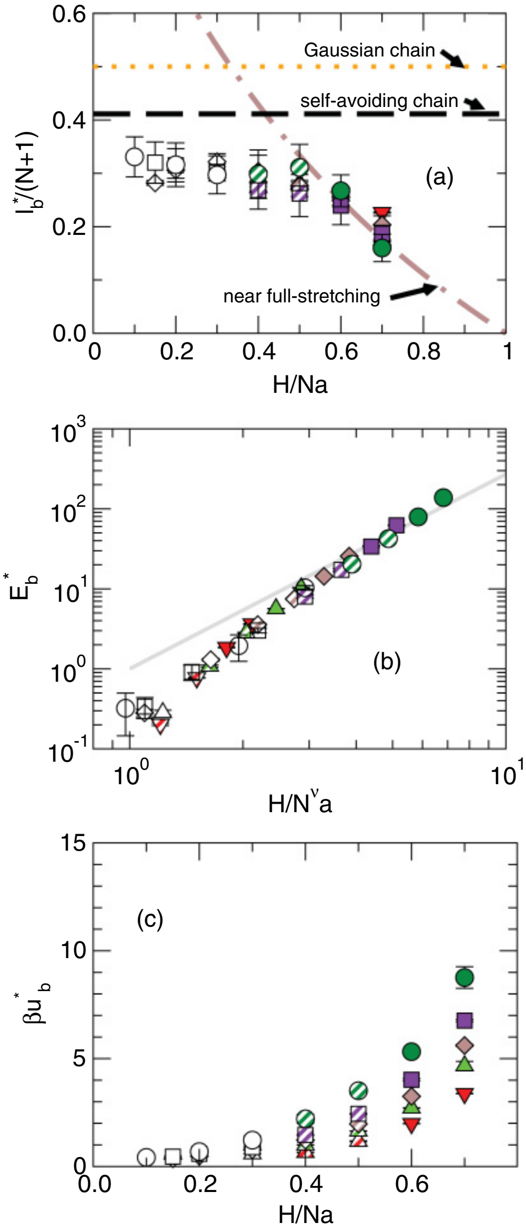

FIG. 5. (Color online) Numerical results for (a) the fraction of monomers near the adsorbing surface at the coil-bridge transition point $l^*_{\rm b}$, (b) the energy barrier between the coil and bridge states at the transition $E^*_{\rm b}$, and (c) the phase boundary described by the reduced energy $\beta u^*_{\rm b}$, as functions of H/a and N. Circles, squares, diamonds, up triangles, and down triangles represent $N = 256, 128, 64, 32$, and 16, respectively. Every data point carries an error bar that was estimated from the analysis of the Z-dependent free-energy curves from ten independent production runs. The dotted and long-dashed lines in (a) indicate universal values predicted from a Gaussian and self-avoiding-chain model (Table I). The dot-dashed curve indicates the qualitative behavior in the asymptotic region, $H/Na \lesssim 1$ (Table I). The straight line in (b) represents a slope of $q = 1/(1-\nu)$, expected from a scaling theory. Data points are further classified: filled symbols for $H/Na = 0.7, 0.6$; shaded symbols for $H/Na = 0.5, 0.4$; and open symbols for $H/Na \leqslant 0.3$.

TABLE I. Fraction of monomers near the adsorption wall, l_b/N, and the reduced adsorption temperature τ_b at the coil-bridge transition point. The results are produced from the scaling theories in Appendixes.

	Gaussian	Self-avoiding		Almost fully stretched
		Weak stretching	Pincus regime	
	$[\nu = \phi = 1/2, q = 2]$	$[\nu = 0.589, q = 2]$	$[\nu = 0.589, q = 1/(1-\nu)]$	
$l_b(H/a,N)/N$	$= 1/2$	$= 0.459$	$= 0.411$	$= (1 - H/Na)/(1 + H/Na)$
$\tau_b(H/a,N)$	$\propto H/Na$	$\propto [(H/N^\nu a)^2/N]^\phi$	$\propto (H/Na)^{q\phi}$	$= (4H/Na)^\phi/(1 - H/Na)^{2\phi}$

At the coil-bridge transition, a polymer needs to overcome the entropic penalty of stretching, in order to make an extended configuration reaching the adsorption surface. This penalty is reflected by a free-energy barrier E_b^*, an example of which is indicated in Fig. 4(b). On the basis of the Pincus scaling for a stretched polymer [11], we expect

$$\beta E_\text{b}^* \sim (H/N^\nu a)^q, \tag{16}$$

where $q = 1/(1-\nu)$ and $\nu = 0.589$ is the scaling exponent for the radius of gyration of a free self-avoiding polymer. Symbols in Fig. 5(b) summarize E_b^* observed for various N and H/Na. The above scaling expectation is plotted in the background as a straight line in a double-logarithmic plot, with the slope reflecting the exponent q. Although a direct agreement is not visible, we can observe an asymptotic behavior. From open triangles and diamonds, to open squares and circles (increasing N), the slope q is asymptotically approached.

Finally, we return to the phase diagram illustrated in Fig. 1(c). The simulation result for the reduced transition energy βu_b^*, determined from the locations of discontinuous jumps presented in Figs. 3(a)–3(j), is plotted as a function of H/Na in Fig. 5(c). Focusing on circles in the plot ($N = 256$), we can see that qualitatively the data agrees with the general trend of the long-dashed curve in the expected phase diagram [Fig. 1(c)]. According to the analysis in Appendix A, the phase boundary in the small H/Na region of Fig. 1(c) can be represented by a power-law exponent $q\phi$; the curve in Fig. 1(c) was produced by using $\phi = 0.5$ [15]. A higher value of ϕ [16] would produce an even stronger scaling exponent $q\phi$. As a function of H/Na, the open circles in Fig. 5(c), however, do not vary as strongly as the expected power law. Another feature in Fig. 5(c) is the presence of N dependence of the phase boundary, whereas according to the analysis in the Appendixes, such dependence should be very weak, if there is any. We attribute these differences to the relatively short chains (up to $N = 256$) simulated in this work—these systems have not reached the asymptotic regimes described by the scaling theory.

IV. SUMMARY

In summary, Monte Carlo simulations that follow a transition probability proportional to the inverse density of states have been employed to study the coil-bridge transition of a grafted self-avoiding polymer. The density of states was determined by an implementation of the Wang-Landau algorithm, in terms of the distance between the center of mass from the grafting point. The usage of such a weight in the Monte Carlo simulations is shown to be an effective tool that determines the large first-order transition gap between the coil and bridge states at the transition point. The numerical results have been analyzed in light of the scaling arguments presented as Appendixes.

ACKNOWLEDGMENTS

The author thanks NSERC for providing financial support and SHARCNET for providing computational time.

APPENDIX A: SCALING THEORY: WEAKLY OR STRONGLY STRETCHED POLYMER

The components of a scaling theory for the current problem can be readily quoted from the literature. A typical bridge conformation contains two segments of the polymer chain, both assumed long: the stem portion of the polymer that has m monomers and is stretched, and a polymer segment of $l = N - m$ monomers ($N,l,m \gg 1$) that is confined near the attractive wall and forms excursion loops. The free energy of the polymer chain, $F(m)$, can then be written in terms of basic parameters in the system,

$$\beta F(m) = C_0 \left(\frac{H/a}{m^\nu}\right)^q - (N - m)|\tau|^{1/\phi}, \tag{A1}$$

where ν is the gyration exponent [17], C_0 a proportionality constant, and $\tau = \beta(u - u_\text{c})$ the reduced energy difference.

The first term describes the entropic penalty of stretching a polymer of length ma over a distance H. For a Gaussian chain, the gyration exponent $\nu = 1/2$ and $q = 2$ [17]; for a self-avoiding chain, the universal gyration exponent has the value [17,18]

$$\nu = 0.589, \tag{A2}$$

and in the weakly stretched polymer regime, $q = 2$ [19]. However, q is not always 2. For a strongly stretched polymer, Pincus has shown that $q = p/\nu$, where p is a scaling exponent [11],

$$p = \nu/(1 - \nu). \tag{A3}$$

A basic assumption in writing down the scaling form for the first term in Eq. (A1), even in the strongly stretched polymer regime, is that $H \ll ma < Na$ [11]. The case of $H \lesssim Na$ corresponds to an almost fully stretched polymer and will be examined in Appendix B.

The second term is written for a large *free* polymer segment adsorbed to the surface of a flat wall near the reduced adsorption energy βu_c. The universal crossover exponent ϕ has the value 1/2 based on a simple mean-field type argument that assumes a uniform monomer density distribution near the surface [17,20]. More accurate theories indicate a different value [20,21]. However, according to a recent Monte Carlo simulation conducted by Metzger *et al.*, $\phi = 0.50 \pm 0.02$ [15]; on the other hand according to a recent analysis performed by Descas *et al.*, $\phi = 0.59$ [16]. The effects of ϕ on the scaling prediction for the coil-bridge transition will be described below.

From the minimization condition $dF/dm = 0$, a relationship between τ and the optimal m can be established,

$$|\tau|^{1/\phi} = C_0 q\nu \frac{(H/a)^q}{m^{q\nu+1}}. \tag{A4}$$

Substituting the relation to the free-energy expression in Eq. (A1) and requiring that the free energy vanishes at the coil-bridge transition yield a simple estimate for the transition point. Denoting l as the number of monomers in the adsorption segment, $l \equiv N - m$, we have

$$\frac{l_b}{N} = \frac{1}{1+q\nu} \tag{A5}$$

at the transition point. Hence, as long as the scaling terms in Eq. (A1) are valid, at the coil-bridge transition, the ratio l_b/N turns out to be a universal constant independent of ϕ and H/Na; this is a strong statement. Eliminating l_b/N from Eq. (A4) yields the relationship between τ, H, and N at the transition,

$$\tau_b{}^{1/\phi} \propto \frac{(H/a)^q}{N^{1+q\nu}}, \tag{A6}$$

a power law depending on ϕ, N, and H/a.

In a Gaussian-chain model, which has $q = 2$ and $\nu = 1/2$, according to Eq. (A5) the ratio $l_b/N = 1/2$; as well, if we adopt $\phi = 1/2$, then the phase boundary becomes $\tau_b \propto H/Na$. Both expressions return to the prediction made earlier by Leermakers and Gorbunov [1], and are summarized in the second column of Table I.

In a model where the excluded-volume effects are considered, $\nu = 0.589$. In the regime of a weakly stretched polymer, $q = 2$, we have $l_b/N = 0.459$ and $\tau_b \propto [(H/a)^2/N^{1+2\nu}]^\phi$. In the regime of a strongly stretched polymer (Pincus regime), $q = 1/(1-\nu)$, we have

$$l_b/N = 0.411, \tag{A7}$$

which is plotted as a long-dashed line in Fig. 5(a). As well, we can express the phase boundary by a power law,

$$\tau_b \equiv \beta u_b - \beta u_c \propto (H/Na)^{q\phi}. \tag{A8}$$

The segment labeled "Pincus regime" in the phase diagram, Fig. 1(c), illustrates βu_b following this power law, where it is further assumed that $\beta u_c = 0.45$ (which is approximately the critical u estimated from a surface adsorption simulation, not presented here). The third and fourth columns in Table I summarize these expressions.

APPENDIX B: SCALING THEORY: ALMOST FULLY STRETCHED POLYMER

In the scaling analysis presented in Appendix A, the validity of the first term in Eq. (A1) depends on the assumption that the stretching distance H is much smaller than the total contour length ma [11],

$$H \ll ma. \tag{B1}$$

Unfortunately some data points presented in this work correspond to a ratio H/Na that falls outside this inequality. The question then becomes: in the parameter regime where the polymer stem is almost fully stretched, what qualitative behavior do we expect to see at the coil-bridge transition?

To answer this question, we must realize that in an almost fully extended configuration, the excluded-volume interaction between the monomers has little effect and can be neglected. The first term in Eq. (A1) can then be replaced by the entropic penalty for a strongly stretched wormlike chain [22],

$$\beta F(m) = \frac{m}{1 - H/ma} - (N-m)|\tau|^{1/\phi}. \tag{B2}$$

Minimizing $F(m)$ with respect to m yields a new relationship between τ and m,

$$|\tau|^{1/\phi} = \frac{2H/ma - 1}{(1 - H/ma)^2}. \tag{B3}$$

This relationship, together with the requirement that at the coil-bridge transition the free energy must vanish, yields

$$\frac{l_b}{N} = \frac{1 - H/Na}{1 + H/Na}, \tag{B4}$$

a result that now depends on H/Na. The prediction for the phase boundary becomes

$$|\tau_b|^{1/\phi} = \frac{4H/N}{(1 - H/Na)^2} \tag{B5}$$

after Eq. (B4) is substituted back to Eq. (B3). Both expressions are summarized in the last column of Table I.

This prediction for l_b/N, as H/Na asymptotically approaches 1, is plotted as a dot-dashed curve in Fig. 5(a). The qualitative estimate for the phase boundary, Eq. (B5), is also plotted in Fig. 1(c). Together with the prediction that l_b/N is a constant discussed in Appendix A, which is valid for weak H/Na, the overall H/Na dependence of l_b/N starts to emerge. Indeed, the results from the Monte Carlo simulations in this work qualitatively agree with the predicted tendencies.

---

[1] F. A. M. Leermakers and A. A. Gorbunov, Macromolecules **35**, 8640 (2002).

[2] T. J. Senden, J.-M. di Meglio, and P. Auroy, Eur. Phys. J. B **3**, 211 (1998).

[3] C. Ortiz and G. Hadziioannou, Macromolecules **32**, 780 (1999).

[4] M. Maaloum and A. Courvoisier, Macromolecules **32**, 4989 (1999).

[5] T. Hugel, M. Grosholz, H. Clausen-Schaumann, A. Pfau, H. Gaub, and M. Seitz, Macromolecules **34**, 1039 (2001).

[6] M. I. Giannotti and G. J. Vancso, Chem. Phys. Chem. **8**, 2290 (2007).

[7] L. Sonnenberg, Y. Luo, H. Schlaad, M. Seitz, H. Colfen, and H. E. Gaub, J. Am. Chem. Soc. **129**, 15364 (2007).

[8] S. Bhattacharya, A. Milchev, V. G. Rostiashvili, and T. A. Vilgis, Eur. Phys. J. E **29**, 285 (2009).

[9] H.-P. Hsu, K. Binder, L. I. Klushin, and A. M. Skvortsov, Phys. Rev. E **76**, 021108 (2007).

[10] H.-P. Hsu, K. Binder, L. I. Klushin, and A. M. Skvortsov, Phys. Rev. E **78**, 041803 (2008).

[11] P. Pincus, Macromolecules **9**, 386 (1976).

[12] F. Wang and D. P. Landau, Phys. Rev. Lett. **86**, 2050 (2001).

[13] F. Wang and D. P. Landau, Phys. Rev. E **64**, 056101 (2001).

[14] N. Metropolis, A. W. Rosenbluth, M. N. Rosenbluth, A. H. Teller, and E. Teller, J. Chem. Phys. **21**, 1087 (1953).

[15] S. Metzger, M. Müller, K. Binder, and J. Baschnagel, Macromol. Theory Simul. **11**, 985 (2002).

[16] R. Descas, J.-U. Sommer, and A. Blumen, Macromol. Theory Simul. **17**, 429 (2008).

[17] P.-G. de Gennes, *Scaling Concepts in Polymer Physics* (Cornell University Press, Ithaca, NY, 1979).

[18] J. C. Le Guillou and J. Zinn-Justin, Phys. Rev. Lett. **39**, 95 (1977).

[19] M. Doi and S. F. Edwards, *The Theory of Polymer Dynamics* (Oxford University Press, Oxford, 1988).

[20] E. Eisenriegler, *Polymers Near Surfaces* (World Scientific, Singapore, 1993).

[21] H. W. Diehl and S. Dietrich, Phys. Rev. B **24**, 2878 (1981).

[22] A. Yu. Grosberg and A. R. Khokhlov, *Statistical Physics of Macromolecules* (American Institute of Physics, NY, 1994).